Analytical and Bioanalytical Chemistry
https://doi.org/10.1007/s00216-018-1424-9

PAPER IN FOREFRONT

An aptamer biosensor for leukemia marker mRNA detection based on polymerase-assisted signal amplification and aggregation of illuminator

Meng Zhang[1] · Fenyue Zhou[1] · Deqi Zhou[2] · Dongli Chen[1] · Hong Hai[1] · Jianping Li[1]

Received: 7 August 2018 / Revised: 27 September 2018 / Accepted: 9 October 2018

Abstract

A novel electrochemical luminescence (ECL) aptamer biosensor via polymerase amplification is constructed for label-free detection of leukemia marker mRNA (miR-16). In order to achieve the ultrasensitive detection of the target mRNA, the cyclic target chain displacement polymerization of leukemia marker mRNA assisted with Klenow fragment of DNA polymerase is employed. The determination is carried out by recording the ECL emission of pyridine ruthenium ($Ru(bpy)_3^{2+}$) complexes embedded into the assistance DNA (ADNA) loaded on the nanogold surface, after the hybridization reaction between the probe DNA (PDNA) and the remaining sequence of the CP's stem part, and the formation of a core-shell sun-like structure. The mercapto-modified capture DNA (CP) is immobilized on the surface of a magneto-controlled glassy carbon electrode by Au-S bond. The CP is opened and hybridized with the target mRNA to form double-stranded DNA. In the presence of polymerase, primer DNA, and bases (dNTPs), the primer chain gets access to its complementary sequence of the stem part and then triggers a polymerization of the DNA strand, leading to the release of mRNA and starting the next polymerization cycle. Finally, the composite of PDNA-covered and ADNA-covered (embedded with $Ru(bpy)_3^{2+}$) gold nanoparticles (hereafter called AuNPs@(PDNA+ADNA-$Ru(bpy)_3^{2+}$) is added, and the ECL intensity is recorded. Because of the polymerization cycle and the aggregation of the illuminator of $Ru(bpy)_3^{2+}$, the detected signal is amplified significantly. The results showed that the corresponding ECL signal has a good linear relationship with a logarithm of target mRNA concentration in the range of 1×10^{-16} to 1×10^{-7} mol/L, with a detection limit of 4.3×10^{-17} mol/L. The mRNA spiked in the human serum sample is determined, and the recoveries are from 97.2 to 102.0%. This sensor demonstrates good selectivity, stability, and reproducibility.

Keywords Aptamer sensor · Polymerase · Electrochemiluminescence · Label-free · Cyclic amplification · Aggregation effect

Introduction

Leukemia is a disease characterized as having the highest morbidity and mortality of all hematopoietic malignancies due to its nature of cloning human hematopoietic stem cells [1, 2]. With a high degree of heterogeneity and incorporation of malignant tumors, patients of this disease usually face life-threatening outcomes [3]. Conventional methods to diagnose leukemia routinely involve blood tests [4], bone marrow examinations [5], and cytogenetic methods [6]. However, the drawbacks of those traditional methods such as procedural complications and impractical testing equipment for clinical use have limited further development. In contrast, the most current development of nucleotide sequence specificity method has been associated with many areas of research including diagnostics and forensic medicine [7, 8]. Several studies have

Electronic supplementary material The online version of this article (https://doi.org/10.1007/s00216-018-1424-9) contains supplementary material, which is available to authorized users.

✉ Hong Hai
583776610@qq.com

✉ Jianping Li
likianping@263.net

[1] Guangxi Key Laboratory of Electrochemical and Magnetochemical Functional Materials, College of Chemistry and Bioengineering, Guilin University of Technology, Guilin 541004, China

[2] College of Biological Sciences, University of California – Davis, Davis, CA 95616, USA

Published online: 29 October 2018

also found mRNA expression to be closely related to many types of tumors as a diagnostic biomarker as well as a potential therapeutic target [9, 10]. As a result, the detection of mRNA [11, 12] has become an important basis for diagnosing and treating clinical tumors, and specifically, regarding leukemia, the qualitative detection of the leukemia marker gene miR-16 can be crucial for early diagnosis [13].

The current method of RNA detection is Northern blotting [14]. This method is considered the standard for mRNA analysis, but the method's procedural complexity limits its utilization in practice. Other methods such as real-time polymerase chain reaction (RT-PCR) [15, 16] and microarray analysis [17, 18] are simple and direct alternatives to detect mRNA. However, these methods are also restricted, such as requiring expensive instruments and complex processes.

In contrast, electrochemical aptamer-based sensing has become one of the most attractive ways to ultrasensitive mRNA detection due to its advantages of inexpensive operation, efficient detection, thorough selectivity, and high accuracy [19–22]. However, the electrochemical DNA biosensors reported often record the signals of the labels marked on the probe DNA and have the disadvantages of a complicated process, especially limiting the improvement of the sensitivities due to the false signals generated by the background signal. It is a hot topic to develop a method of improving the sensitivity of electrochemical aptamer biosensors.

In this paper, a novel polymerase-assisted cyclic electrochemiluminescence aptamer biosensor is proposed for the ultrasensitive detection of the leukemia marker gene mRNA. With the combination of the polymerase-assisted signal amplification and the illuminator aggregation in AuNPs@(PDNA+ADNA-Ru(bpy)$_3^{2+}$), the detection sensitivity of the sensor is greatly increased. The method has high sensitivity and good selectivity for the marker gene mRNA of leukemia determination and can provide a reference for early diagnosis and treatment of leukemia.

Experiments

Apparatus and reagents

MPI-E electrochemiluminescence analysis system (Xi'an Ruimai Analytical Instruments Co., Ltd.); PGSTAT128N Auto lab electrochemical workstation (Swiss Wantong Limited); AL204 Electronic Analytical Balance (METTLER TOLEDO Instrument Co., Ltd.); DF-101S collector temperature heating magnetic stirrer (Jintan City, Jiangsu Province, Jinxiang Long Electronics Co., Ltd.); KS-120EII type ultrasonic cleaning machine (Ningbo Haishu Branch Health Equipment Co., Ltd.); CHI660D electrochemical workstation (Shanghai Chenhua Instrument Co., Ltd.).

$FeCl_3·6H_2O$ and $FeSO_4·7H_2O$ are purchased from Aladdin (Shanghai, China); KCl, NaOH, NaCl, Tris-HCl buffer, tris (2-carboxyethyl) phosphine (TCEP), mercaptoethanol (MCH), ethylenediaminetetraacetic acid (EDTA), pyridine ruthenium, and *N*,*N*-dipropyl-1-propanamine (TPA) are purchased from Aladdin Company (Shanghai, China); $Na_2HPO_4·12H_2O$ and $NaH_2PO_4·2H_2O$ are purchased from the West Long Chemical Co., Ltd. Reagents used are of analytical grade. PBS solution ($Na_2HPO_4·12H_2O$ 11.6037 g, $NaH_2PO_4·2H_2O$ 1.1850 g) and TE buffer (10 mmol/L Tris-HCl, 1 mmol/L EDTA, 100 mmol/L NaCl, pH 7.8) are bought from Aladdin (Shanghai, China); Klenow fragment polymerase (2.5 U/μL), 10 × enzyme reaction buffer (500 mmol/L Tris-HCl, 50 mmol/L $MgCl_2$, 10 mmol/L DTT), and deoxyribonucleic acid mixture (dNTP Mix) are purchased from Shanghai Bioengineering Engineering Company. The sequences of the oligos are listed in the Electronic Supplementary Material (ESM) Table S1. The experimental water was double-distilled water.

The preparation of the Fe_3O_4@Au magnetic nanoparticles

Preparation of the Fe_3O_4@Au magnetic nanoparticles follows the method used in a previous study [23] with slight modification, where 1.14 g $FeCl_3·6H_2O$ and 0.67 g $FeSO_4·7H_2O$ are weighed and dissolved in 250 mL of double-distilled water. The mixture is then poured into a three-neck flask protected by a consistent input of nitrogen. After rapid stirring and continual N_2 supply for 1.5 h at 50 °C, 2 mol/L NaOH is added to ensure the pH level of the solution remained 10. Afterwards, the solution is heated to 80 °C for 30 min while maintaining the pH level and then washed several times with double-distilled water and absolute ethyl alcohol to achieve neutrality. The solution is then diluted to a concentration of 5 mg/L Fe_3O_4 solution and stored at 4 °C for use later.

0.229 g sodium citrate is dissolved in 100 mL of double-distilled water and is poured into a 250-mL three-neck flask, then heated under stirring. While the solution is being stirred and heated to 90 °C, 1 mL of the prepared Fe_3O_4 magnetic nanoparticles and 2 mL of 10 mmol/L chloroauric acid solution are quickly added. The stirring also continued for 15 min after the heat source is removed. Magnetic separation is performed after the wine-red solution cooled to room temperature. Double-distilled water is then used to wash the solution several times until the solution is neutral and also to dilute the solution to 20 mL. The solution is then stored at 4 °C for later use.

The preparation of AuNPs

Preparation of AuNPs is the same as the previous study [24]. All glassware to be used are cleaned with freshly prepared aqua regia before testing and then repeatedly washed with

distilled water and allowed to dry naturally, and then, 1 mL of $HAuCl_4 \cdot 3H_2O$ (1%) solution and 99 mL of distilled water are added to a 250-mL three-neck flask. After adding 3 mL of sodium citrate buffer (1%) along with vigorous mechanical stirring, the color gradually changed into wine. The solution is then boiled for 30 min, cooled to room temperature, and stored at 4 °C.

The preparation of AuNPs@(PDNA+ADNA-Ru(bpy)$_3^{2+}$)

0.02 g of pyridine ruthenium is added to 1 mL of TE buffer. One milliliter AuNPs solution, 200 μL ADNA, and 50 μL PDNA are then added to the mixture, mixed completely under ultrasound conditions. The solution is kept at room temperature for 1 h to obtain the AuNPs@(PDNA+ADNA-Ru(bpy)$_3^{2+}$) solution and stored at 4 °C for later use.

Procedures of assay

The magneto-controlled glassy carbon electrode is polished with a 0.03-μm diameter alumina powder, and the impurities adhering to the surface of the electrode are removed through ultrasonic cleaning with double-distilled water and ethanol for 5 min. In the 0.05 mol/L $[Fe(CN)_6]^{3-/4-}$ working solution, the electrode potential is measured by an electrochemical workstation, where the scanning potential is adjusted to a range of − 0.2–0.6 V and the scanning speed is 0.05 V/s. The sulfhydrylation of CP is carried out by mixing 0.1 mL of 1 μmol/L CP with 10 μL of 10 mmol/L TCEP for 2 h. The sulfhydrylation CP is then mixed with 1 mL of Fe_3O_4@Au magnetic nanoparticle solution. After 24 h at 37 °C, the CP self-assembled through the Au-S bond and the addition of 100 μL of 1 mmol/L mercaptohexanol solution followed by 1 h of incubation is to ensure CP from participating in nonspecific adsorption. After 25 min of centrifugation (15,000 r/min), the resulting supernatant is discarded, and the pellet is resuspended in TE buffer to obtain Fe_3O_4@Au/capture DNA solution.

The treated magneto-controlled glassy carbon electrode is immersed in the solution of 10 μL Fe_3O_4@Au/capture DNA (1-DNA) and 40 μL of 1 mol/L TE buffer solution. 1-DNA is self-assembled on the electrode surface by the Au-S bond and incubated at 37 °C for 12 h. In order to further reduce nonspecific adsorption of 1-DNA onto the electrode surface, blank binding sites of the unfixed capture DNA on the electrode surface are closed to reduce the background signal, and the electrode is immersed in 1 mmol/L mercaptohexanol and incubated at 37 °C for 1 h. Afterwards, different concentrations of the target mRNA are added, and the solution is incubated at 37 °C for 1 h. In the presence of the target mRNA, the CP and mRNA complementarily hybridized allowing the hairpin structure to open. The modified electrode is then placed within a 10x enzyme reaction buffer solution (50 μL) containing primer DNA (1 μmol/L), Klenow fragment polymerase (5 U), dNTP mix (50 μmol/L), and TE buffer solution (40 μL) and afterwards incubated for 2 h at 37 °C. The primer DNA hybridized with the complementary sequence at the bottom of the hairpin neck. After adding the polymerase and base, the primer DNA started to amplify and proceeded to replace the target mRNA. The replaced target mRNA is then returned to open another hairpin to reset and prepare for another cycle. Finally, the above electrode is immersed in the AuNPs@(PDNA+ADNA-Ru(bpy)$_3^{2+}$) (20 μL) and is allowed to react for 1 h at 37 °C in order to achieve the desired modified electrode. Then, the modified electrode described above is washed three times with TE buffer solution and double-distilled water, respectively, to wash off any unconnected materials for further measurements. The schematic diagram is shown in Fig. 1.

Electrochemical luminescence signal detection

The modified electrode is used as the working electrode, the platinum wire electrode as the counter electrode, the Ag/AgCl (saturated KCl) electrode as the reference electrode, and the PBS solution (0.2 mol/L, pH = 7.4 containing 0.1 mol/L of TPA) is used as the working solution. The ECL signal is detected by MPI-E Electroluminescence Analysis System with cyclic voltammetry with the scanning potential ranging from 0~1.25 V and scanning speed of 0.1 V/s. The voltage of the photomultiplier tube is 900 V.

Results and discussions

Characterization of the electrode modification process

Figure 2 illustrates the cyclic voltammogram changes of the magneto-controlled glassy carbon electrode during the modification of different materials. Cyclic voltammetry is carried out in 0.05 mol/L $[Fe(CN)_6]^{3-/4-}$ solution. Figure 2(a) is the curve of the bare electrode which has the highest current signal. Figure 2(b) is of a curve which shows a current reduction when Fe_3O_4@Au is immobilized on the bare electrode. Figure 2(c) shows the curve of the electrode modified with CP and MCH which also resulted in a reduction of current signal due to a reduction of the electrode surface self-assembled by CP.

Adding to the target mRNA led to a significant increase in the coverage of the DNA phosphoric acid skeleton to the electrode surface, which also led to a significant decrease in the current (curve d). When added with polymerase, base, primer DNA, and enzyme buffer, a 5′ to 3′ direction primer extension allows the target mRNA to replace and further open another CP for another cycle of displacement, then inevitably

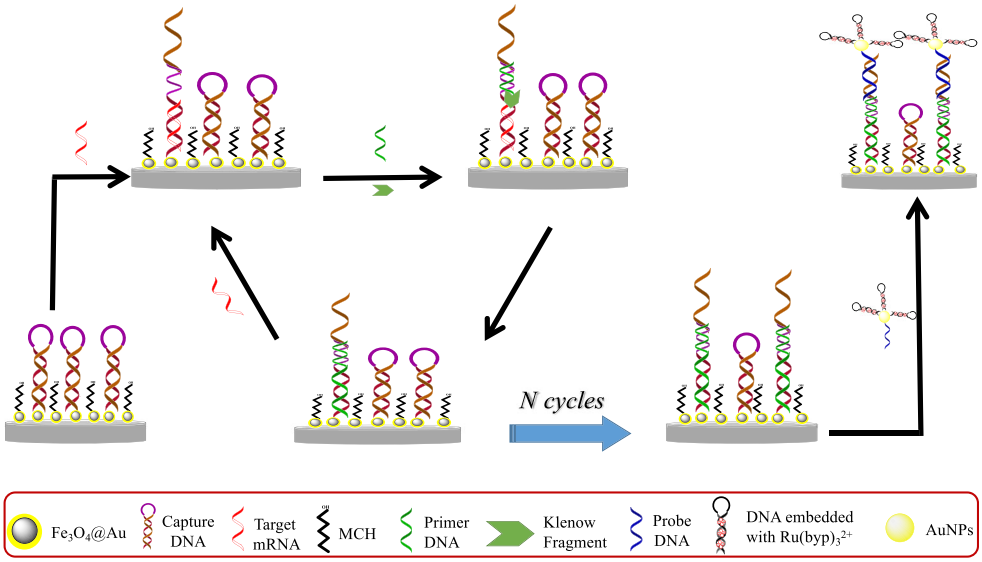

Fig. 1 Detection of leukemia based on polymerase-assisted label-free electrochemiluminescence DNA biosensor

results in the current to significantly reduce (curve e). With the addition of AuNPs@(PDNA+ADNA-Ru(bpy)$_3^{2+}$), the redox current also reduced due to the blocking of the electron transport after pyridine ruthenium-embedded into dsDNA combined with gold nanoparticle hybridizes (curve f).

Figure 3 shows the variations in the AC impedance of the electrodes among the different step modifications of different substances. As the figure illustrates, the bare glassy carbon electrode has a minimum resistance value (Fig. 3(a)), and then the resistance of the Fe_3O_4@Au modified electrode increases (Fig. 3(b)). After self-assembled with CP via Au-S bond and blocking with MCH on Fe_3O_4@Au, the resistance increased further (Fig. 3(c)). When the target mRNA hybridization occurred, the resistance increased (Fig. 3(d)). When polymerase, base, and primer DNA are added, the new chains formed by replication replace the target mRNA, and the resistance increases correspondingly to the previous step (Fig. 3(e)). Finally, in the presence of AuNPs@(PDNA+ADNA-Ru(bpy)$_3^{2+}$), the largest resistance can be seen due to further hindering of electron transfer (Fig. 3(f)).

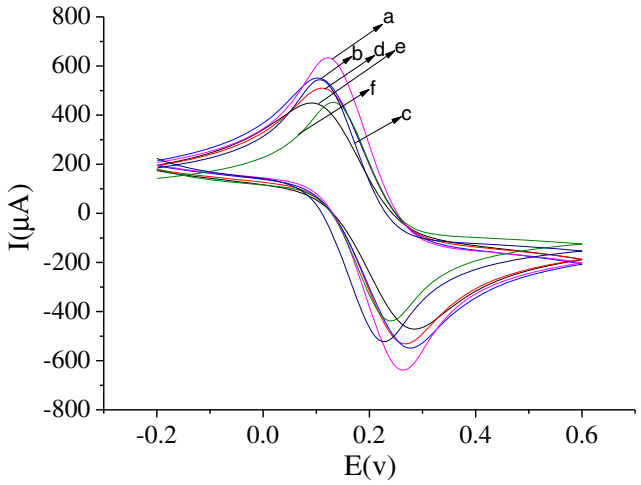

Fig. 2 Cyclic voltammograms of different processes on modified electrode CVs of the different electrodes in 0.05 mol/L $[Fe(CN)_6]^{3-/4-}$ (a) bare electrode; (b) Fe_3O_4@Au/(a); (c) CP/MCH/(b); (d) mRNA/(c); (e) polymerase/(d); (f) AuNPs@(PDNA+ADNA-Ru(bpy)$_3^{2+}$)/(e); scan rate: 0.1 V/s

Optimization of experimental conditions

Hybridization time is a factor that affects the efficiency of hybridization. Hybridization time of the target mRNA with CP is optimized and depicted in Fig. 4. As shown in Fig. 4(a), the ECL signal gradually increases with the hybridization time and then reaches a platform at 60 min, indicating the completion of the hybridization between the complementary mRNA and CP. As a result, the hybridization time is selected

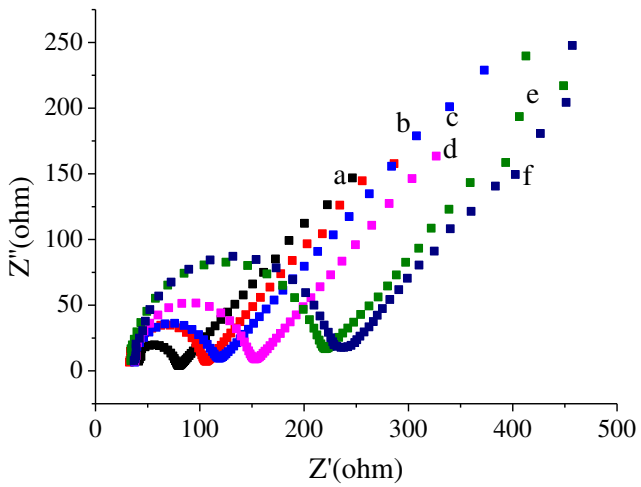

Fig. 3 Ac impedances characterization of the different electrodes in 0.05 mol/L $[Fe(CN)_6]^{3-/4-}$ (a) bare electrode; (b) Fe_3O_4@Au /(a); (c) CP /MCH/(b); (d) mRNA/(c); (e) polymerase/(d); (f) AuNPs@(PDNA+ADNA-Ru(bpy)$_3^{2+}$)/(e); scan rate: 0.1 V/s

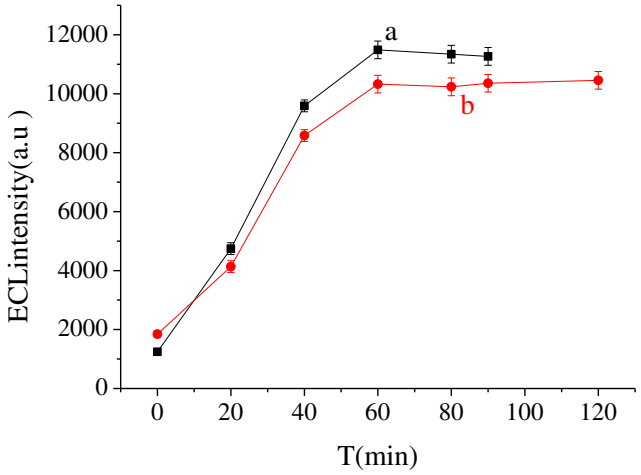

Fig. 4 Optimization of mRNA hybridization time (a) and hybridization time between probe DNA and the CP's stem part (b)

as 60 min. The hybridization reaction time between the probe DNA and the CP's stem part is an important factor in the ECL signal. Figure 4(b) demonstrates that as the reaction time increases, the ECL signal gradually increases and tends to the platform. Therefore, the hybridization time for ECL signal is also 60 min.

In this work, the polymerase is used to enhance the detection signal by recycling the target; the use of polymerase directly affects the sensitivity of the method. Optimizations of the reaction time and the amount of polymerase are carried out. As illustrated in Fig. 5(a), the ECL signal increases with the enzymatic react time, indicating that the polymerase is involved in the circulation of the target DNA hybridization, and the ECL signal gets to the highest value at the reaction time of 2 h. Figure 5(b) shows the ECL signal gradually increasing as the number of enzyme increases while the

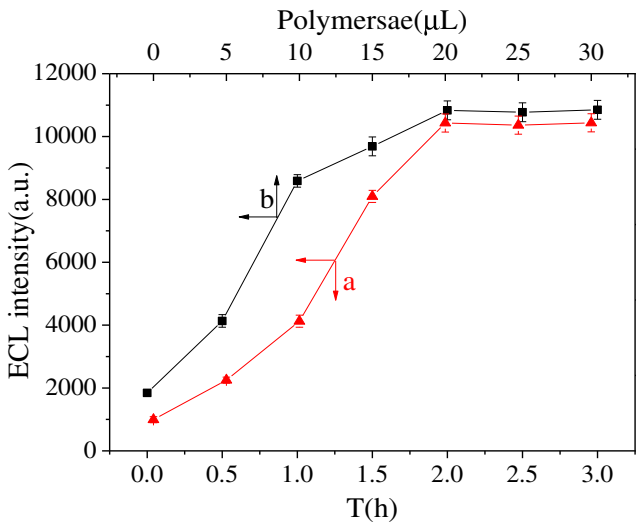

Fig. 5 The optimization of polymerase amount (a) and polymerase reaction time (b)

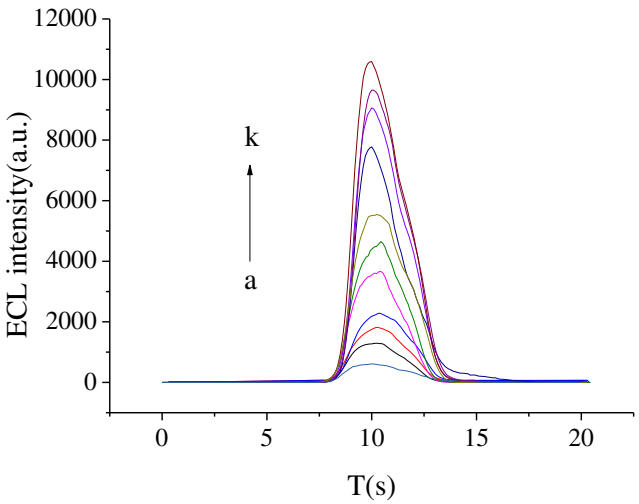

Fig. 6 ECL intensity of biosensor at different mRNA concentrations. From a to k: 0, 10^{-16}, 10^{-15}, 10^{-14}, 10^{-13}, 10^{-12}, 10^{-11}, 10^{-10}, 10^{-9}, 10^{-8}, 10^{-7} mol/L, respectively

luminescence signal tends to be stable when the amount of enzyme used in this experiment is higher than 20 μL.

Calibration curve

Figure 6 shows the electrochemical luminescence curves corresponding to different concentrations of target leukemia mRNA hybridized with the AuNPs@(PDNA+ADNA-$Ru(bpy)_3^{2+}$ labeled CP for 1 h, and Figure 7 illustrates the calibration curve. There is a linear relationship between the ECL intensity (ΔI) and the logarithm of mRNA concentration (log C) in the range of 1.0×10^{-16}–1.0×10^{-7} mol/L. The linear regression equation is $\Delta I = 583.61 + 1200.98$ log C (10^{-16} mol/L) ($r = 0.9988$) with a detection limit of 4.3×10^{-17} mol/L. The comparison of the parameters of the proposed methods and the others is shown in Table 1; this technique has a lower detection limit than other methods [25–28]. The ECL signal is enhanced via the circulating detection of

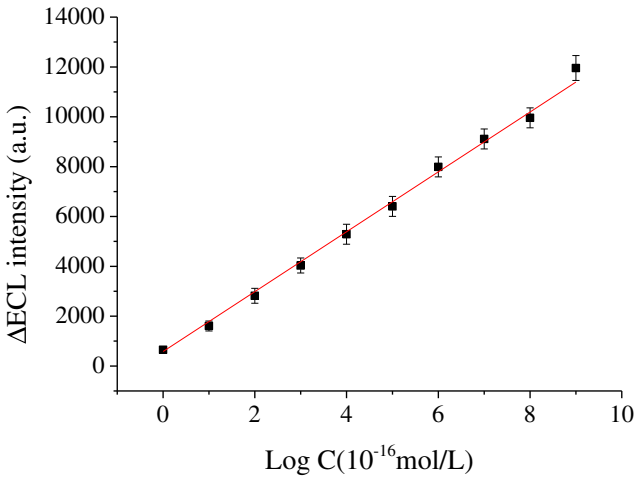

Fig. 7 Linear curves of different concentrations of mRNA

Table 1 Comparison of the proposed method and the other previous methods

Detection methods	Linear range (mol/L)	Detection limit (mol/L)	References
Fluorescence	4.6×10^{-9}~6.7×10^{-8}	7.5×10^{-11}	[25]
Rolling circle amplification (RCA)	2.5×10^{-14}~1.0×10^{-10}	1.5×10^{-14}	[26]
Colorimetry	5.0×10^{-11}~6.0×10^{-9}	5.0×10^{-11}	[27]
Differential pulse voltammetry (DPV)	1.0×10^{-9}~1.0×10^{-13}	4.2×10^{-14}	[28]
Electrochemiluminescence (ECL)	1.0×10^{-16}~1.0×10^{-7}	4.3×10^{-17}	This work

mRNA by a polymerase and effective aggregation of illuminator molecules with AuNPs@(PDNA+ADNA-Ru(bpy)$_3^{2+}$), so the sensitivity of the detection for leukemia mRNA is greatly improved.

Selectivity

In order to evaluate the selectivity of the biosensor, target mRNA , single-base mismatch of mRNA, three-base mismatches of mRNA, and non-complementary strand of mRNA are chosen to hybridize with the capture DNA on the electrode surface. The result is shown in Fig. 8; the ECL intensity increases significantly in response to 1.0×10^{-7} mol/L target mRNA, which means that the single-base mismatch mRNA, three-base mismatch mRNA, and non-complementary mRNA rarely have interference to the detection of target mRNA, proving the biosensor can effectively detect the target with high selectivity.

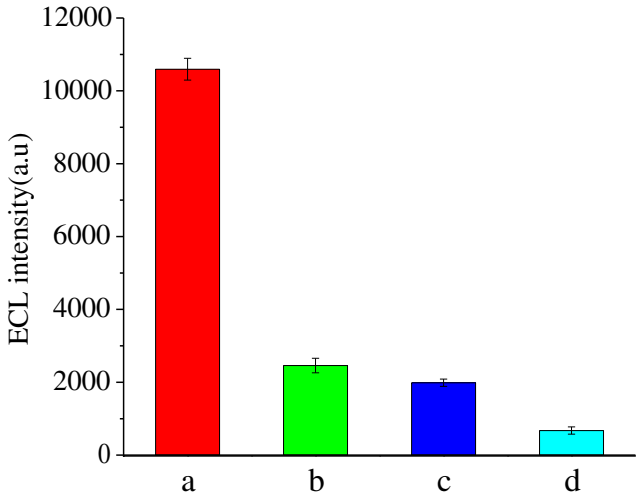

Fig. 8 Selectivity of fabricated DNA biosensor: (a) 1×10^{-7} mol/L mRNA, (b) 1×10^{-7} mol/L single-base mismatched mRNA, (c) 1×10^{-7} mol/L three-base mismatched mRNA, (d) 1×10^{-7} mol/L non-complementary mRNA

Table 2 The analyses of blood samples

Samples	Added (mol/L)	Found (mol/L)	RSD ($n = 5$, %)	Recovery (%)
1	1.00×10^{-12}	1.02×10^{-12}	2.8	102.0
2	1.00×10^{-11}	9.72×10^{-12}	3.2	97.2
3	3.00×10^{-11}	2.95×10^{-11}	3.9	98.3

Reproducibility and stability

When the newly prepared biosensor is stored at 4 °C for 2 weeks, the ECL signal is only reduced by 2.36% when compared with the original values. This result indicates that the sensor has good stability. Under the same conditions, five sensors are prepared to detect 1.0×10^{-7} mol/L mRNA, and the relative standard deviation of the analytical results of the five determinations is approximately 3.67%, which indicates a good reproducibility of the sensor.

Samples analysis

In order to test the practical use of the biosensor, human serum samples are provided by Guilin University of Technology Hospital for testing. The results are shown in Table 2. The recoveries ranged from 97.2% to 102.0% and the RSD is less than 4% indicating that the sensor can be used for practical sample assay.

Conclusions

Herein, we developed an aptamer biosensor and proposed a novel strategy for leukemia marker mRNA label-free detection. The sensitivity is significantly improved due to the polymerase cyclic amplification and the aggregation of the illuminator. This neoteric technique can offer a promising strategy for early diagnosis of cancer marker genes.

Funding information This research is financially supported by the National Natural Science Foundation of China (No.21765006), the Guangxi Natural Science Foundation, China (No. 2015GXNSFFA139005), and the High-Level Innovation Teams of Guangxi Colleges and Universities and Outstanding Scholars Program (Guijiaoren[2014]49).

Compliance with ethical standards

Conflict of interest The authors declare that they have no conflict of interest.

Ethical standards and informed consent The study and experimental sections were approved by the Hospital of Guilin University of Technology. Human serum samples used in this study do not have any identifying information about all the participants that provided written informed consent.

References

1. Musto P, Negrini M, De LL, Cuneo A. Dissecting chronic lymphocytic leukemia with 13q-using microRNA expression profile: editorial for the paper "miRNA expression profile of chronic lymphocytic leukemia patients with 13q deletion". Leuk Res. 2016;47:114–5.
2. Achille NJ, Othus M, Phelam K, Zhang SB, Cooper K, Godwin JE, et al. Association between early promoter-specific DNA methylation changes and outcome in older acute myeloid leukemia patients. Leuk Res. 2016;42:68–74.
3. Buckley SA, Jimenez SD, Othus M, Walter RB, Lee SJ. Quality of life from the perspective of the patient with acute myeloid leukemia. Cancer. 2018;124:145–52.
4. Setiadi A, Owen D, Tsang A, Milner R, Vercautern S. The significance of peripheral blood minimal residual disease to predict early disease response in patients with B–cell acute lymphoblastic leukemia. Int J Lab Hematol. 2016;38:527–34.
5. Boyerinas B, Zafrir M, Yesilkanal AE, Price TT, Hyjek EM, Sipkins DA. Adhesion to osteopontin in the bone marrow niche regulates lymphoblastic leukemia cell dormancy. Blood. 2013;121:4821–31.
6. Jenderny J, Goldmann C, Thede R, Ebrecht M, Korioth F. Detection of clonal aberrations by cytogenetic analysis after different culture methods and by FISH in 129 patients with chronic lymphocytic leukemia. Cytogenet Genome Res. 2014;144:163–8.
7. Esfandyarpour R, Yang L, Koochak Z, Harris JS, Davis RW. Nanoelectronic three-dimensional (3D) nanotip sensing array for real-time, sensitive, label-free sequence specific detection of nucleic acids. Biomed Microdevices. 2016;18:1–10.
8. Kitamura M, Aragane M, Nakamura K, Watanabe K, Sasaki Y. Development of loop-mediated isothermal amplification (LAMP) assay for rapid detection of Cannabis sativa. Biol Pharm Bull. 2016;39:1144–9.
9. Zhang M, Hai H, Zhou FY, Zhong JC, Li JP. Electrochemical luminescent DNA sensor based on polymerase-assisted signal amplification. Chin J Anal Chem. 2018;46:203–9.
10. Martens ES, Böttcher R, Croce CM, Jenster G, Visakorpi T, Calin GA. Long noncoding RNA in prostate, bladder, and kidney cancer. Eur Urol. 2014;65:1140–51.
11. Yang LM, Li J, Pan W, Wang HY, Li N, Tang BY. Fluorescence and photoacoustic dual-mode imaging of tumor-related mRNA with a covalent linkage-based DNA nanoprobe. Chem Commun. 2018;54:3656–9.
12. Miao P, Jiang YT, Zhang T, Huang Y, Yang YG. Electrochemical sensing of attomolar miRNA combining cascade strand displacement polymerization and reductant-mediated amplification. Chem Commun. 2018;54:7366–9.
13. Calin GA, Dumitru CD, Shimizu M, Bichi R, Zupo S, Noch E, et al. Frequent deletions and down-regulation of micro-RNA genes miR15 and miR16 at 13q14 in chronic lymphocytic leukemia. Proc Natl Acad Sci. 2002;99:15524–9.
14. Enfield KSS, Martinez VD, Marshall EA, Stewart GL, Kung SH, Enterina JR, et al. Deregulation of small non-coding RNAs at the DLK1-DIO3 imprinted locus predicts lung cancer patient outcome. Oncotarget. 2016;7:80957–66.
15. Yu MM, Yao S, Luo KM, Mu QF, Yu Y, Luo GH, et al. Apolipoprotein M increases the expression of vitamin D receptor mRNA in colorectal cancer cells detected with duplex fluorescence reverse transcription-quantitative polymerase chain reaction. Mol Med Rep. 2017;16:1167–72.
16. Sanyal S, Siriwardena AK, Byers R. Measurement of indicator genes using global complementary DNA (cDNA) amplification, by polyadenylic acid reverse transcriptase polymerase chain reaction (poly A RT-PCR): a feasibility study using paired samples from tissue and ductal juice in patients undergoing pancreatoduodenectomy. Pancreatology. 2018;18:458–62.
17. Lin X, Chen Y. Identification of potentially functional circRNA-miRNA-mRNA regulatory network in hepatocellular carcinoma by integrated microarray analysis. Med Sci Monit. 2018;24:70–8.
18. Ma Y, Shi L, Zheng C. Microarray analysis of lncRNA and mRNA expression profiles in mice with allergic rhinitis. Int J Pediatr Otorhinolaryngol. 2018;104:58–65.
19. Wang S, Zhang LQ, Wan S, Gansiz S, Cui C, Liu Y, et al. Aptasensor with expanded nucleotide using DNA nanotetrahedra for electrochemical detection of cancerous exosomes. ACS Nano. 2017;11:3943–9.
20. Li JP, Sun M, Wei XP, Zhang LM, Zhang Y. An electrochemical aptamer biosensor based on "gate-controlled" effect using β-cyclodextrin for ultra-sensitive detection of trace mercury. Biosens Bioelectron. 2015;74:423–6.
21. Zhou FY, Hai H, Yuan YL, Li JP. Ultrasensitive electrochemiluminescence biosensor for mRNA based on polymerase assisted signal amplification. Electroanalysis. 2017;29:983–9.
22. Qin GX, Zhao SL, Huang Y, Jiang J, Liu YM. A sensitive gold nanoparticles sensing platform based on resonance energy transfer for chemiluminescence light on detection of biomolecules. Biosens Bioelectron. 2013;46:119–23.
23. Wang LP, Huang YB, Lai YH. Surface enhanced Raman scattering activity of dual-functional Fe_3O_4/Au composites. Appl Surf Sci. 2018;435:290–6.
24. Yao Y, Xue M, Zhang ZB, Zhang MM, Wang Y, Huang FH. Gold nanoparticles stabilized by an amphiphilic pillar [5] arene: preparation, self-assembly into composite microtubes in water and application in green catalysis. Chem Sci. 2013;4:3667–72.
25. Ding QW, Zhan QQ, Zhou XM, Zhang T, Xing D. Theranostic upconversion nanobeacons for tumor mRNA ratiometric fluorescence detection and imaging-monitored drug delivery. Small. 2016;12:5944–53.
26. Ali MM, Li F, Zhang ZQ, Zhang KX, Kang DK, Ankrum JA, et al. Rolling circle amplification: a versatile tool for chemical biology, materials science and medicine. Chem Soc Rev. 2014;43:3324–41.
27. Alsage OA, Kumar S, Zhu BC, Sejdic JT, McNatty KP, Hodgkiss JM. Ultrasensitive colorimetric detection of 17β-estradiol: the effect of shortening DNA aptamer sequences. Anal Chem. 2015;87:4201–9.
28. Zhao FL, Xie QY, Xu MF, Wang SY, Zhou JY, Liu F. RNA aptamer based electrochemical biosensor for sensitive and selective detection of cAMP. Biosens Bioelectron. 2015;66:238–43.

Meng Zhang is a master's student from Guilin University of Technology in China and he is mainly engaged in bioanalysis and electrochemiluminescence biosensor research. The electrochemiluminescence biosensors are applied to the accurate detection of cancers.

Dongli Chen is a master's student from Guilin University of Technology in China and she is mainly engaged in electroanalytical chemistry and chemical biosensors research. The research is applied to the detection of genetically modified crops.

Fenyue Zhou is a master's student from Guilin University of Technology in China and she is mainly engaged in bioanalysis and electrochemiluminescence biosensor research. The electrochemiluminescence biosensors are mainly used for cancer and heavy-metal-ion detection.

Hong Hai is Professor of the Department of Bioengineering, Guilin University of Technology, and Council Member of the Guangxi Chemical Society. He has been developing scientific works in bioanalysis and biosensor research for several years. This research is applied to cancer analysis and other works.

Deqi Zhou is an undergraduate student from the University of California – Davis, studying Biochemistry and Molecular Biology. He is especially involved in areas of health and medical science. He has been an academic tutor as well as a medical service provider and wishes to continue gaining experience and develop a career in the field.

Jianping Li is Professor at the College of Chemistry and Bioengineering, Guilin University of Technology. He received his bachelor and master degrees from Jilin University in 1988 and 1991, respectively, and his PhD degree from Zhejiang University in 2003. His research focuses on chemical and biological sensors and bioassays.